ELSEVIER

Nuclear Instruments and Methods in Physics Research A 488 (2002) 517–535

NUCLEAR INSTRUMENTS & METHODS IN PHYSICS RESEARCH Section A

www.elsevier.com/locate/nima

Muon tracking detector for the air shower experiment KASCADE

P. Doll[a,*], W. Bartl[b], C. Büttner[a], K. Daumiller[c], K.H. Kampert[a,c], H.O. Klages[a], D. Martello[d], R. Obenland[a], L. Pentchev[e], J. Zabierowski[f]

[a] *Institut für Kernphysik, Forschungszentrum Karlsruhe, 76021 Karlsruhe, Germany*
[b] *Institut für Hochenergiephysik der Ö.A.W., 1050 Wien, Austria*
[c] *Institut für Experimentelle Kernphysik, Universität Karlsruhe , 76021 Karlsruhe, Germany*
[d] *Department of Physics, University of Lecce, 73100 Lecce, Italy*
[e] *Institute for Nuclear Research and Nuclear Energy, 1784 Sofia, Bulgaria*
[f] *The Andrzej Soltan Institute for Nuclear Studies, 90950 Lodz, Poland*

Received 14 January 2002; received in revised form 11 February 2002; accepted 11 February 2002

Abstract

A large area streamer tube detector, located within the KASCADE experiment, has been built with the aim to identify muons and their directions from extensive air showers by track measurements under more than 18 r.l. shielding. 1000 streamer tube chambers of 4 m length have been produced and tested. The detector concept is presented. The influence of the design and operational factors on the detector performance are shown. Various approaches to determine the angular resolution of the muon tracking detector are discussed.

1. Introduction

Ultra High Energy (UHE) astrophysics deals with the investigation of UHE cosmic ray particles (above 10^{15} eV), which interact with the nuclei of the atmosphere and create Extensive Air Showers (EAS). However, at UHE their flux is much below 10^{-5} s^{-1} m^{-2}. Therefore, instead of direct measurements in space, ground-based experiments of large detection area must be used. To understand the nature of the UHE particles it is indispensable to measure as many components of the cascade developing in the atmosphere as possible. Particularly important is the measurement of the muon component of the EAS, because some of the muons reaching the observation level carry information about the very first interactions at the top of the atmosphere. In particular, the investigation of muon angles in EAS with respect to the shower direction [1] can be used for studying the mass composition of the primary cosmic rays. Such an angle can be transformed into the Muon Production Height (MPH) taking into account the corresponding shower core distance [2]. For large distances from the shower core reliable triangulation of individual muon tracks provides information on the MPH and helps to identify the nature of the primary UHE particle. Monte Carlo (MC)

*Corresponding author. Tel.: +49-7247-82-4171; fax: +49-7247-82-4047.
E-mail address: doll@ik.fzk.de (P. Doll).

0168-9002/02/$ - see front matter
PII: S0168-9002(02)00560-0

calculations show that by means of the MPH parameter, for a good statistics of showers, heavy primary particles like iron nuclei can be distinguished from medium mass particles or light ones, like protons.

As a subsystem to the KASCADE experiment [3] a large area Muon Tracking Detector (MTD) consisting out of Streamer Tube (ST) chambers was put into operation. KASCADE at the *Forschungszentrum Karlsruhe* is taking data since 1996, measuring various shower parameters with a $200 \times 200\ m^2$ scintillator array and a central detector, consisting of a hadron calorimeter and muon detectors. The new MTD of about $500\ m^2$ sr is intended to track the muons above 0.8 GeV created in EAS. In addition, it will enhance the capability of KASCADE in measurement of the muon multiplicities and their lateral distributions. The MTD will also allow to perform systematic studies on cosmic ray muons like those compiled by Allkofer et al. [4].

In the past, various tracking detectors for measuring cosmic ray particles have been put into operation either on the surface of the earth [5–8] or deep underground [9–11]. The surface arrays emphasize the aspect that position sensitive detectors, which measure the angle of each track, may be used to improve the precision in the measurement of the primary particle direction, because the directions of muons are much better correlated with the primary cosmic ray direction than any other secondary particle component in an EAS [7]. Tracking modules made from planes of STs have been applied to the observation of EAS in the PLASTEX experiment [8]. Very large detectors consisting out of ST or Geiger counters have been set up in the Gran Sasso Tunnel [9,10], and Frejus Tunnel [11], respectively. All three detectors can be defined as underground observatories with the intriguing objectives of studying very high energy muons and neutrinos from stellar collapse and searching for point-like sources of gammas or neutrinos of very high-energy.

Main parameters of a muon tracking detector, as seen at the early prototyping stage, were described in Ref. [12]. The present paper is a detailed presentation of the complete MTD. First, the specially developed STs are described together with the extensive tests after production. The influence of environmental and design factors on the ST performance is shown. Next, the presentation of the complete detector system, its geometry and readout electronics follows and the results of various tests of the MTD are given. Finally, methods to investigate the efficiency and angular accuracy of the detector are presented.

2. KASCADE streamer tubes

Intensive studies [12,13] with various commercial STs [14,15] and custom-made tubes [16,17] for the air shower experiment KASCADE indicated that this type of detector [18] is well suited for particle density measurements in air showers and for track measurements of penetrating particles.

In the prototyping phase the advantage of using conductive PVC for the STs was confirmed. In close collaboration with the company WATECH [19], having experience in extruding conductive PVC comb profiles [20], many design details have been elaborated. They concerned, e.g., the use of the high resistive covers for the open ST profiles [21]. A large effort was put into the reduction of the dark current. For this purpose the anodes were made out of high-quality copper-beryllium wire of 100 μm diameter, tempered and smoothed by evaporating ≈ 0.3 μm of silver onto the wire surface, with a copper flash under the silver [22].

The first leak tests as well as the High Voltage (HV) conditioning of the ST chambers have been carried out on the site of the factory using pure carbondioxide as chamber gas to avoid build up of gas radicals during conditioning.

2.1. ST chamber design

Concerning the detector dimensions, a ST chamber houses 16 anode wires in two cathode comb profiles, extruded for eight parallel ST cells of $9 \times 9\ mm^2$ cross-section and 4000 mm length. For the comb profiles the high resistivity PVC of well-defined conductivity was obtained from very clean PVC by doping it with carbon powder before extrusion [20]. To close the electric field around the anode wire effectively [21] when applying

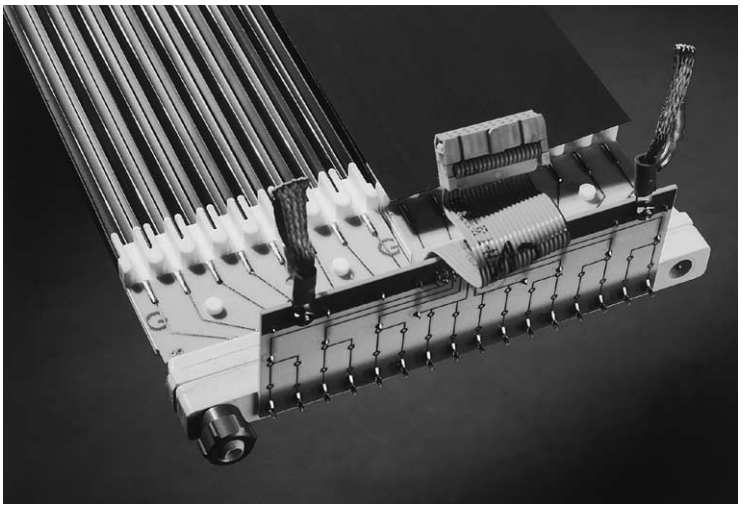

Fig. 1. Detailed view of an opened ST chamber with installed adapter board.

negative HV to the cathode profiles, a bakelite sheet cover was employed.

The tolerance of the ST cell geometry was required to be less than 0.1 mm. To each comb profile end-pieces were glued, which carry the printed circuit boards, onto which the anode wires are soldered. The wires are supported by spacers every 500 mm. The wire tension before soldering was adjusted according to the room temperature of the detector assembling hall and amounts to 3 N at 20°. The copper-beryllium wire has an expansion coefficient about 3 times smaller than the PVC material. The temperature in the detector building varies by $\pm 5^{\circ}$ over a year period. Consequently, the wire tension changes with temperature by ± 0.22 N, what translates into ∓ 9 μm change in the wire sagging between the spacers from its nominal 42 μm value (electrostatic force is ignored). The comb profiles, together with the mounted wires, were slid into PVC envelopes, which were sealed off with endcaps exhibiting connectors for anode wires, HV and gas. Details of the ST chamber design are shown in Fig. 1 and its main technical parameters are summarized in Table 1.

Table 1
ST chamber design parameters

PVC profile resistivity	$10^5\ \Omega/\square$
Bakelite cover resistivity	$10^{11}\ \Omega$ cm
Anode wire diameter	100 μm
Anode wire tension	3 N at 20°C
Wire sagging between spacers	42 μm
ST chamber dimensions	$13 \times 166.6 \times 4000$ mm^3

2.2. Acceptance tests

When the ST chambers arrived at the *Forschungszentrum Karlsruhe* they were individually tested for gas leaks. Each chamber was put under 20 cm of water equivalent overpressure with argon and closed off for 2 h. The change in the height of the water column is due to the real gas loss of the closed system and environmental pressure and temperature variations. These parameters were monitored to correct any change in the water column due to these environmental variations. From these measurements the effective loss in units of chamber volumes per year was calculated, normalized to a 5 mbar operation overpressure in the air shower experiment. A compilation for all 1000 chambers shows, that 85% out of them exhibit a leak rate of less than one chamber volume per year. The remaining chambers exhibit also a tolerable leaking.

After the leak test the ST chambers were mounted on tables in groups of 12 and flushed in parallel with a specific isobutan/argon gas mixture.

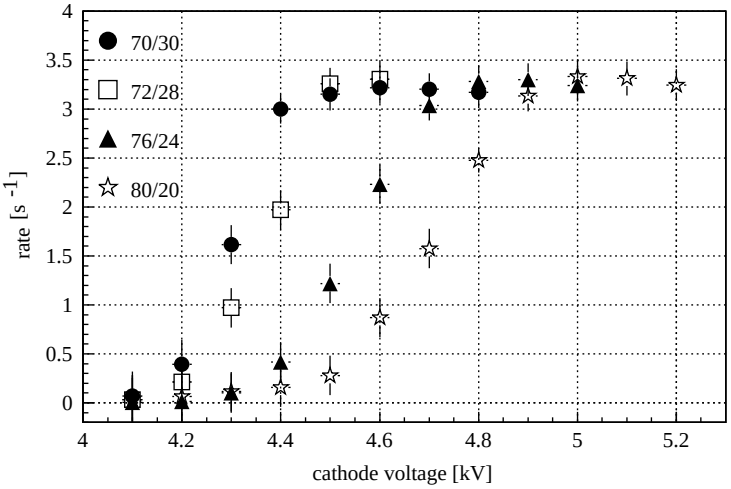

Fig. 2. Count-rate plateaus for various isobutan/argon gas mixtures. Numbers quoted are in volume percent.

This flushing replaced the argon being used in the leak test. Fig. 2 shows the count rate plateau for a chamber for various gas mixture settings.

The results in Fig. 2 were obtained by measuring the integral rate in the pulse height spectra from a ST chamber, however, gated with a plastic scintillator telescope. We continued to test the chambers, with the lowest isobutan admixture, to avoid during the conditioning phase deposition of organic radicals on the electrodes of the detectors. On those test tables the chambers were read out by a prototype readout electronic chain (see Section 3.2) recording the hits on the wires and on pick-up strips, which have been arranged perpendicularly to the wires, with a pitch of 20 mm and width of 18 mm. For checking the homogenity of the response of the ST chambers, the amplitudes on the anode wires from penetrating cosmic ray particles were recorded. The ST chambers had been operated always at the same HV in the plateau region (see Fig. 2). In Fig. 3, the results of such measurements, however ungated, are given, showing the variation of the mean pulse height across a module area of 2×4 m^2, consisting out of 12 chambers which employ 192 wires and 192 perpendicular strips. Such a survey was obtained within 2 h. For the observed variation of the mean pulse height the following reason may be responsible. The fresh detectors contain still some impurities and therefore, exhibit spurious discharge signals of various amplitudes. This has an influence on the mean ADC values shown in Fig. 3 because the threshold settings of the comparators in the readout chain (see Section 3.2) can be equalized only with a finite precision.

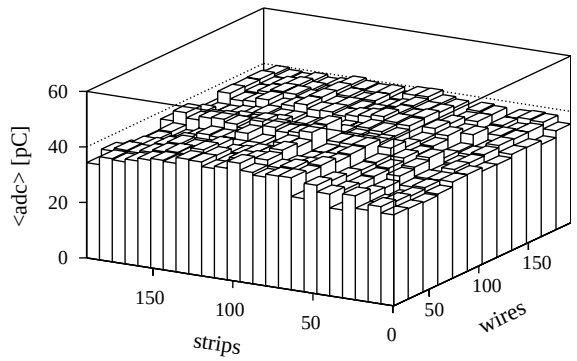

Fig. 3. Variation of the mean pulse height across a module of 2×4 m^2 area.

To investigate the homogenity of the ST chambers in closer regions of several strip pitch units, the wire amplitude spectrum was divided into components recorded in coincidence with varying number of influence strips as shown in Fig. 4. The number of influence strips, mainly determined by the spatial extension and orientation of the discharge in the ST wire cell is called *cluster size*. The integral intensities in these different wire amplitude spectra follow the

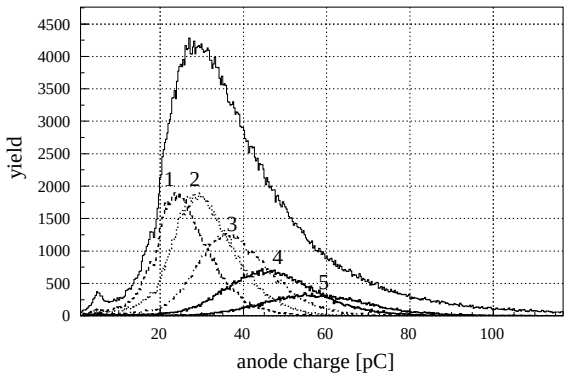

Fig. 4. Anode wire amplitude spectrum divided into contributions of different cluster sizes (1–5) on the pick-up strips placed perpendicularly above the chamber.

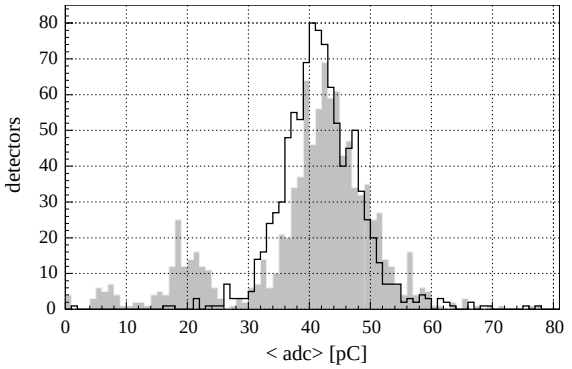

Fig. 5. Variation of the mean anode wire pulse height for 1000 chambers before (grey) and after (solid line) corrections for different operation conditions.

geometrical spread of the influence charge on the strips and depend also on the amount of charge coupling through the bakelite sheet and chamber envelope onto the strips.

The production and test period for 1000 ST chambers lasted for several months. During this period changes in the gas mixture, operation temperature and gas pressure in the laboratory occurred. To obtain a survey of the mean pulse height of all chambers we corrected their anode wire pulse height distribution for these parameters, which have been monitored during the runs. In Fig. 5, the distribution of the mean anode wire pulse height is presented. The structure around 20 pC is due to a comparatively higher gas pressure situation. The spread of the corrected distribution may be due to operational variations in the recurring setup of gas and electrical connections as well as variations in the geometry of the chambers. During the first operation, the fresh chambers exhibited varying integral count rates due to the incomplete conditioning. These rates have also been corrected for the operation conditions.

3. Description of the MTD

The MTD is located within the KASCADE experiment (Fig. 6) in the $5.4 \times 2.4 \times 44\ m^3$ tunnel, buried in the ground under a shielding of 18 r.l., made of concrete, iron and soil. This corresponds to about three hadronic interaction lengths. A multilayer of six iron plates of 3 cm thickness, separated each by 5 cm sand, absorbs a large fraction of low-energy electromagnetic particles, thus enhancing the identification of the muon tracks with an energy exceeding 0.8 GeV. The MTD extends almost in north–south direction with a declination of 14.9° to the east. The MTD centre is 54.65 m north from the centre of the KASCADE scintillator array. The level of the middle modules in detector towers (see below) is 1.70 m below the array detector level. The location of the MTD supports the detection of muons exhibiting some transverse momentum with respect to the hadrons being detected in the hadron calorimeter [23], which houses itself additional muon detectors, operating at different muon energy thresholds.

The ST chambers described above are grouped in, so-called, *modules*. Four modules, three positioned on horizontal planes (top, middle, bottom) and one arranged vertically (wall), form a muon telescope called *detector tower*. The whole detector comprises 16 towers arranged in two rows. In the photo of the complete MTD in the tunnel (Fig. 7) the tower structure is clearly seen.

3.1. Detector module and tower

A detector module of the size $2 \times 4\ m^2$ consists of 12 ST chambers, which are described in

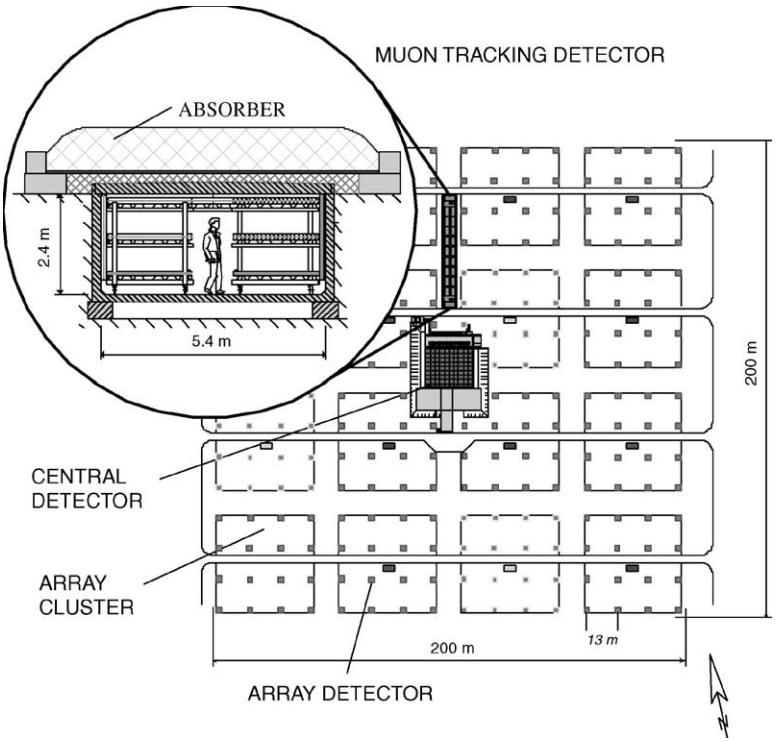

Fig. 6. Layout of KASCADE experiment with a vertical section across the MTD detector presented in an inset.

Fig. 7. The MTD in the tunnel.

Section 2.1. Above the ST chambers there is a layer of a rigid polyester foil of 75 μm thickness with evaporated aluminium strips [24] (about 0.1 mg/cm^2) of 20 mm pitch (18 mm width) and 2 m length, perpendicular to the wires. Another layer of such foil is mounted below the ST chambers but with strips oriented diagonally at an angle of 30° with respect to the wire direction.

These *diagonal strips* are made out of the same strip material but two strips are combined at the readout side. The total resistivity of a *perpendicular strip* is 47–53 Ω depending on the aluminium thickness and varies between 15 and 65 Ω for a diagonal strip pair, depending on the length. The electrical contact with the strips is achieved by screwing a broad zinc coated washer together with the polyester foil onto a rigid PVC board. Onto the silver-coated screws further adapter boards are soldered for enabling connection to the readout electronics.

As shown in Fig. 1, two neighbouring ST wire cells are combined on the adapter board, thus giving four wire signals out of one 8-cell comb profile. The chambers, together with the strip foils, are sandwiched between two layers of high-density styrofoam (25 mm from above and 50 mm from below) and are resting on a thin (0.7 mm) but rigid steel structure. In a detector tower horizontal modules are spaced vertically by 820 mm—from wire plane to wire plane. The vertical (wall) module enhances the angle acceptance of the MTD and allows to investigate very inclined showers. Additional detector modules and/or absorber planes can be installed in between the horizontally arranged modules.

The gas supply system is arranged as follows. In a temperature stabilized container outside the tunnel 50 l gas bottles provide argon and isobutan (initially also carbon dioxide) at a pressure of 1.5 bar each. These gases flow to the gas mixer in the tunnel. Before entering the gas mixer, membrane valves allow a fine tuning of the pressure of each gas component. Gas flow meters, after each membrane valve and before the mixer, monitor the gas composition. The partial pressures of each gas component add in the gas mixer volume. The gas leaves the mixer unit and is distributed into 16 channels using 16 needle valves. Each channel supplies one tower, where the gas runs in series through all chambers of the top module, then the middle module, next the bottom one and, finally, the wall module. With a gas flow of 0.5 dm^3/h for one tower (240 dm^3 volume), the gas is there exchanged after about 20 days, which is sufficient because of the small leakage of the detectors and small radiation load in the shielded tunnel. The total length of the gas system, for all ST chambers in series, amounts to almost 200 m for each tower.

3.2. Readout and data acquisition electronics

We are using a chain-type readout system, commonly used with large-scale ST detectors [25,26]. The readout electronics can be subdivided into three levels. The first level in the readout structure is the front-end electronics, consisting of boards for 32 inputs, mounted to the detector modules and acquiring signals from wires and strips. Each module provides signals from 96 wire pairs, 192 perpendicular and 96 diagonal strips. The total number of readout channels in 16 detector towers amounts to 24 576. The front-end boards generate out of the strip and wire pulses digital signals being used for track reconstruction. A logical OR of wire signals (DIGOR) within one board is used for trigger purposes. In addition, an analog sum (ANOR) of the combined wire signals for 4 ST chambers (one board) is produced. The ANOR spectra are useful information, being supplementary to the hit pattern data.

Each module requires three *wire boards* and nine *strip boards* for readout. Twenty-four boards for two module combinations (bottom + middle or top + wall) are interconnected in series by means of a 20-conductor ribbon cable, thus forming a serial readout chain structure. Such a chain is connected to the dedicated intermediate electronic module, called *Splitter Board* (SB) which forms a second level of the readout structure. Four of such SBs occupy one crate and provide the interface for two detector towers. By means of these SBs, operating with optical couplers for the bus signals, the digital ground of the readout chain is separated from the CAMAC digital ground. These SBs are of our custom design, however, they are functionally compatible with CAEN SY480 modules, in order to match the CAEN C267 Streamer Tube Acquisition System (STAS) controllers, used in the setup.

One CAMAC and one VME crate contain the third level electronics. The CAMAC crate contains four C267 STAS modules plus several 2249A LeCroy ADCs for the ANOR signals. The VME crate communicates with the CAMAC system via

CES 8210 CAMAC Branch Driver and houses trigger electronics, controller for CAEN HV System, ADC for monitoring parameters like temperature, gas pressure and flow, and the Transputer based VME Controller (TVC) [27] for communication via optical links with the central host in the KASCADE data acquisition system.

3.2.1. Front-end and trigger electronics

Front-end readout electronics for the MTD is designed in the form of boards, which follow the 32 channel architecture, developed by SGS Thomson [28] as IP32 cards. Subdivision into 32 channels per board matches our detector requirements. The detailed information on the board design can be found in Ref. [29]. The idea of the front-end electronics board for chain readout consists of conversion of each analog signal from wires or strips, which exceeds predefined threshold, into digital binary information ("hit" or "no hit"). This binary information, under certain triggering conditions, is loaded in parallel into a 32-bit long shift register. Connecting 24 boards in a chain, as in our case, creates a 768-bit long register, from which data are shifted out, via the bus, with the clock frequency of 4 MHz into the STAS controller during readout cycle. The physical length of a 24 boards chain amounts to about 24 m. Signals from wires and from strips are of the opposite polarity and of different amplitudes. Therefore, two types of boards were developed: one for wires and one for strips.

The tests and tuning of the 850 strip and wire readout boards were performed using a Qbasic program on a PC. By means of a special interface board the program provided control and test signals via the parallel port of the PC. For testing the shift registers a programmed 8-bit word was shifted through a chain of a given number of boards many times, and each time at the output compared with the input word. All amplifier channels were checked using the *test-even* and *test-odd* lines, available on the boards. Along these lines the monoflops of one board can be triggered for all 16 even or 16 odd channels.

For the purpose of triggering of the MTD a custom-made Trigger Unit (TU) was designed. It is a MTD specific modification of the module used for KASCADE scintillator array [30]. The two trigger modes are possible: *internal* and *external* one. For internal triggering a multiplicity combination of DIGOR signals from wire boards of all towers is used. Any value of this multiplicity in the range from 1 to 48 can be preset by software. Specific combinations allow to study special muon directions. For instance, all bottom modules amount to 48 trigger sources. As external trigger sources other KASCADE detector components like the Array, the Top Cluster or the Trigger Plane are used. While the internal trigger registers muons down to the tunnel shielding energy threshold the array trigger for shower energies above 10^{14} eV provides comparatively more high-energy muons. The time window in which all ST signals exceeding the electronic threshold will be stored, extends to 4 μs after the trigger event.

One of the important tasks of the TU is the generation of the Time Label (TL) for each event. Such TLs are generated also in other parts of the KASCADE experiment and are used by acquisition software (central event builder) to build an air shower event from data supplied by various detector components. With every event also an actual time is being stored. It is derived from a central GPS controlled clock system of KASCADE at the start-up of the MTD and then, incremented locally in the TU by centrally distributed 1 Hz precise clock signals. With the TL every absolute trigger time is recorded with 200 ns precision.

3.2.2. Event handling

Whenever a trigger condition (see Section 3.2.1) is fulfilled in the TU, an EVENT signal is sent to the TVC and, in addition, a NIM-pulse is generated. On receiving the EVENT Signal, the TVC locks the TU, thus inhibiting more triggers and reads out the TL and trigger registers.

The NIM-pulse is split and fed into the START inputs of all STAS modules. The STAS first sends a signal (LOAD), which moves the data from the comparators into the shift-registers of the front-end boards. Then clock pulses are applied which shift the data along the chain into the memory of

the STAS. Upon completion of the readout the first STAS in the CAMAC crate produces a Look At Me (LAM) signal which is fed into an external interrupt input of a CAMAC Branch Driver CBD8210 to generate a VME-interrupt. This interrupt causes a high priority process of the TVC to scan all STAS and ADC modules for LAM signals and to transfer the data into the memory of the TVC. When this task is completed the TU is unlocked and a low priority process preprocesses the data and sends them, via a second TVC over TCP/IP, to the central event builder.

The high priority Data Acquisition Program (DAQ) [31] coordinates the experiment control, time and event handling and data storage. It uses C-routines on TVC, which initialize the hardware: the VME and CAMAC crates, the TU, the STAS controllers and the ADC modules. For this initialization an experiment set-up file, structured similar to Windows .ini files, is read. It contains the addresses of the crates, of the STAS and the ADC modules in the crate and the number of each readout chain for a given STAS module. Readout chains are subdivided in subchains, each corresponding to a group of readout boards for the wires and strips, respectively. While the event acquisition is performed with high priority, the data transfer from TVC memory to the central event builder is done with low priority. Monitor histograms of various parameters are also allocated and filled with low priority. These histograms are continuously accumulated and can be viewed online with a separate program. They allow to perform immediate checks when doing adjustments of threshold and timing settings on the front-end boards.

The different data blocks (TU, STAS and ADC data) are combined into one large block and sent to the central event builder. The raw data are analysed with the help of a program package, which reads the data files, calculates the hit positions using the geometry Data Base (DB), reconstructs the particle directions and merges information from all KASCADE detector components.

In Table 2, the basic operational parameters of the MTD are listed.

Table 2
Operational parameters of the MTD

Detector telescopes (towers)	16
Modules per tower	3 horiz. + 1 vert.
Detecting surface for vertical muons	128 m^2
Total detecting surface	512 m^2
Number of ST chambers	768
Number of readout channels	24 576
—wire pairs	6 144
—strips	18 432
Number of readout boards	768
Gas mixture (final)	70% isobutan + 30% argon
Gas flow rate/tower	0.5 dm^3/h
Full MTD gas volume	240 $dm^3 \times 16 =$ 3840 dm^3

4. Environmental tests

The MTD experiences over a period of 1 year temperature variations from 16°C to 26°C (almost no day/night variations) and pressure changes from 990 to 1040 mbar. These parameters influence the operation of the gas detectors. In Fig. 8, the dark current behaviour of the upper module of one tower (192 wires) during the period from June 1998 (day 151) until May 1999 (day 485) is shown. The average dark current of 330 nA corresponds almost to the rate of the penetrating particles, taking into account the high gas gain of the streamer mechanism. We observe the following dependencies: +17 nA/°C and +2.5 nA/% humidity and −2.5 nA/mbar. The dependence on the humidity of the air in the underground tunnel is due to leakage currents around the HV connectors. The temperature and pressure changes modify also the amplitudes in the STs, which are continuously recorded.

Since the gas system is open to the outside atmosphere, variations in the detector amplification of 0.4%/mbar, as shown in Fig. 9, pertain to variations in the atmospheric pressure. The structures seen in the smooth decline of amplification with increasing atmospheric pressure are probably due to minor variations in the gas composition, of about 1%, stimulated by rapid pressure changes of several mbar/h and which may have occurred few days before because of the small flow rate. For employing the drift time

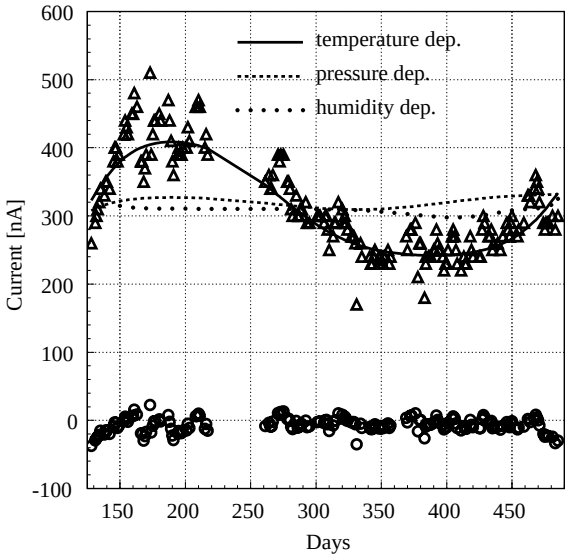

Fig. 8. Dark current (△) drawn by upper module of one tower and its dependence on temperature, pressure and humidity. Constant current values for 12 chambers (◦) are reached after correction for these dependences (shifted in the plot by −330 nA).

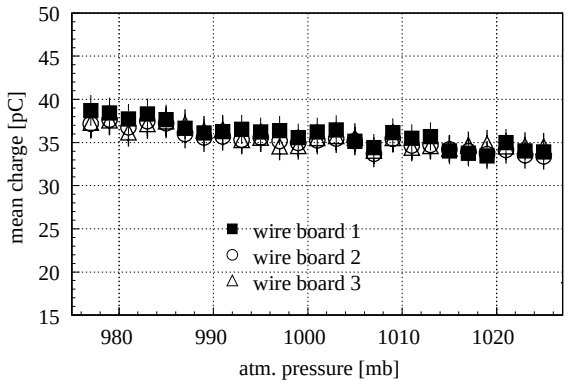

Fig. 9. Mean charge amplitude in a tower recorded by the three wire boards of the bottom module as a function of the atmospheric pressure.

measurement in the future, such variations should be minimized, by improving the gas flow regulation.

To avoid ageing effects during the start-up phase, the detectors were operated with $Ar + CO_2$ (10% + 90%) and next with a gas mixture consisting out of 10% argon, 40% isobutan and 50% carbondioxide. In the course of time, the isobutan content was further increased and finally replaced the carbondioxide resulting in an improved spatial confinement of the streamer charge distribution. When introducing the 40% of isobutan it was observed that the anode wire charge signal became smaller by a factor of about 2 but the hit efficiency increased from around 60% for $Ar + CO_2$ to around 90% (see below). The reason for the increase of the efficiency is probably due to the reduced cluster size along the wire and strip readout chain, respectively. A gas containing isobutan quenches the discharges, leading to less fluctuating signals in space and time.

5. Efficiency

While the efficiency of the ST chambers was investigated by employing a precisely aligned plastic scintillator telescope (see Fig. 2), the efficiency of the detector modules in a tower was determined by means of the following procedure. The track finding algorithm looks within the range of one cluster size first for the *3-hit* tracks which are tracks with hits in three modules. Thereafter, the algorithm looks for the *2-hit* tracks, using for these the hits in two modules, not utilized by the 3-hit tracks. Having then the starting coordinate and direction of each particle, however, ignoring tracks which point outside the tower, the data along the wire and strip readout chain are checked, within a defined cluster size range, for wire and strip entries along those particle tracks. The ratio of the total number of found hits to the number of expected ones gives the efficiency values for wires and strips (perpendicular or diagonal) in different modules, respectively. A result of such a procedure for bottom modules in all 16 towers is given in Fig. 10. The efficiency (averaged for all wires and all strips along a module) of larger than 0.9 for the wires is also measured for all other modules of the MTD. For vertical tracks the geometrical limit of the efficiency amounts to 90%. Inclined tracks are more abundant and lead to larger efficiency values. The diagonal strips seem to exhibit a systematically smaller efficiency, which is probably related to the double width (larger

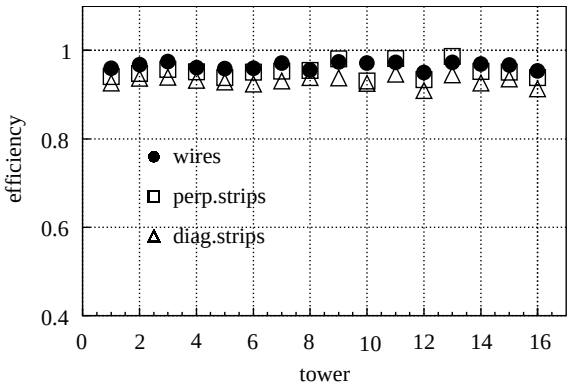

Fig. 10. Mean efficiency of the bottom module for all towers separately, for wires, perpendicular and diagonal strips.

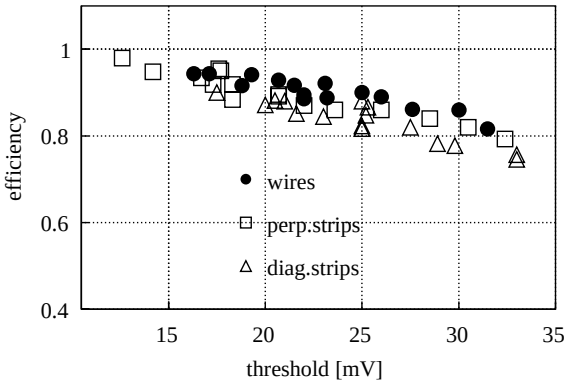

Fig. 11. Mean efficiency versus threshold voltage of the top modules for the wires, perpendicular and diagonal strips.

capacity) of the diagonal strips compared to the perpendicular ones and which can be accounted for by lower threshold settings. Hit efficiencies in all three modules lead to an average track efficiency of about 73%.

The dependence of the efficiency on the threshold voltage on the readout boards was investigated. Fig. 11 gives the results for the top modules of all towers for wires, perpendicular and diagonal strips. On average, one observes $-1\%/\mathrm{mV}$ efficiency change over a 20 mV range. During long-term operation the threshold values, however, remain stable within ± 0.1 mV for several days. In the full range of temperature changes from 16°C to 26°C over a 1 year cycle the threshold temperature coefficient amounts to $-0.2\ \mathrm{mV}/^{\circ}\mathrm{C}$.

6. MTD angular resolution

6.1. Geometry checks

The precise knowledge of the MTD geometry is of primary importance for the reconstruction of the tracks and has direct influence on the detector angular resolution. The positions of the strips and wires have been measured using optical and mechanical tools with respect to the corners of each module. The centre of each module was determined with respect to the reference system of the tunnel having its origin in the centre, the Y-axis along the long side (almost north, see Fig. 6) and the X-axis along the short side (almost east) of the tunnel. The Z-axis is oriented towards the zenith and the array scintillator detector level is taken as $Z = 0$. Each of these measurements has a precision of $\sigma \leqslant 1.5$ mm. The zenith angle of the infalling particle starts from the Z-axis, the azimuth angle starts from the north and increases to the east. All the coordinates of wires and strips are stored in the geometry DB. The direct measurement might be affected by systematic errors in the positioning of the tools used, therefore, the geometry has been verified with independent techniques, involving cosmic muons.

6.1.1. Event selection criteria

For the verification of the detector geometry the sample of collected tracks has been used. Only tracks generated by high-energy muons ($E_\mu >$ few tens of GeV) should be considered. Such muons are produced in the upper layers of the atmosphere, they may be nearly parallel and well aligned with the shower direction. CORSIKA simulations [32] show that muons produced ~ 8 km above sea level and with energies larger than 30 GeV form an average angle with the shower direction of less than 0.3°. However, in the data sample there is some fraction of tracks exhibiting comparatively large angles with respect to the shower axis, which may originate from particles with low energy or result from the reconstruction algorithm in a high particle density environment. These have to be rejected.

First of all, we have accepted 3-hit tracks with a χ^2-like track quality parameter Q lower than 2.5.

This parameter is defined as

$$Q^2 = \sum_{i=1}^{3} \frac{D_{\mathrm{tr}}^2(\mathrm{Hit}_i)}{A_{\mathrm{Hit}_i}}$$

where $D_{\mathrm{tr}}(\mathrm{Hit}_i)$ is the distance in space between the hit and the track coordinate and A_{Hit_i} is the area $(\mathrm{d}x \times \mathrm{d}y)$ of the hit (*wire cluster size* × *strip cluster size*). The so defined track quality is not a standard χ^2 because we have used the reciprocal of the area of the hit as a weight of the square of the hit–track distance but it has a similar behaviour. This track quality cut rejects with high efficiency accidental tracks without reducing significantly the particle track sample. Fig. 12 shows the distribution of the track quality for tracks with a zenith angle of less than 18° and with fixed cluster size (solid symbols) $\mathrm{d}x, \mathrm{d}y = 20$ mm (minimum possible for strip cluster size) and, therefore, fixed denominator in the equation for the track quality. Structures in the Q distribution are due to the granularity of the detector modules. The Q parameter exhibits the following features. When the distance to the shower core becomes smaller the particle density in the MTD becomes larger. The Q values become somewhat larger for muon tracks close to the shower core probably due to the effect of overlapping clusters near to the shower core. Inclined tracks lead also to larger wire and strip clusters, however, even larger D_{tr} values and therefore larger Q values. It should be recognized that a very large cluster size, results in a small Q, which should also be excluded for high-quality tracks.

Fig. 13 shows the variation of the mean cluster size of signals from wire pairs and perpendicular strips as a function of zenith angle of the track, averaged over azimuth angles. For almost vertical tracks only one wire pair is employed with a geometrical width of 20 mm. The mean cluster size exceeds 20 mm, which is due to a finite crosstalk between neighbouring wire cells and/or the electronic channels (about 3%). On average, the influence charge is induced on several strips of 20 mm pitch.

Investigation of the angle in space Ψ between the shower direction and track in the MTD as a function of the distance of this track to the shower core shows, that for distances smaller than 20 m comparatively large angles Ψ are observed. They probably stem from wrongly reconstructed tracks due to the higher density of hits. Therefore, a distance cut of 20 m from the shower core was used in the analysis.

Concerning the air shower data supplied by the KASCADE scintillator array, we accepted for our analyses only events with the core reconstructed in a fiducial area of 90 m around its centre [33]. The so-called truncated number of muons [34] reconstructed from the scintillator array data, together with the electron size of the shower, provides a good measure of the shower energy E_0 [35]. Close

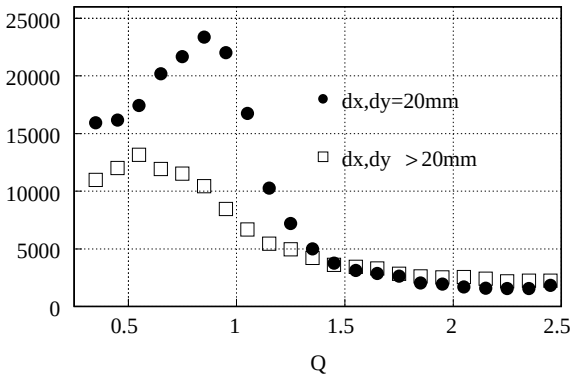

Fig. 12. Track quality Q distribution for small and large cluster sizes.

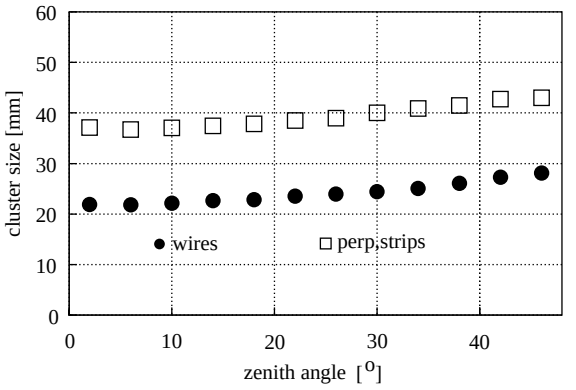

Fig. 13. Mean cluster size for wires and perpendicular strips as a function of zenith angle.

to the shower detection threshold of the array ($\approx 10^{14}$ eV), the shower energy E_0 may be of reduced accuracy.

6.1.2. Internal geometry of each module

At first, the internal geometry of each module has been checked, by using event configurations in which only one wire pair and one strip in each strip plane (*perpendicular* and *diagonal*) had signals. Assuming that the X and Y positions have been measured correctly with respect to the corners of the module, one can minimize the distance of any X, Y hit to its closest diagonal strip and improve the geometry DB for the diagonal strips. In this way, one has the possibility to identify (and to eliminate) both a systematic offset of the diagonal strip plane with respect to the X, Y hits and a systematic rotation of the diagonal strips plane with respect to its nominal (30.0°) orientation.

Fig. 14 shows mean deviations of distances between the X, Y crossing point and the nearest diagonal strip. Adjustment of the overall diagonal strip position allows to obtain a narrow distribution centered nearly at zero. There remains certain staggering of the displacement, which is observed to be correlated with the orientation of the diagonal strips in the modules. These deviations are being investigated and will be further minimized in the future.

6.1.3. Alignment checks with cosmic ray particles

The first method, commonly used for verification of the geometry of a tracking apparatus, consists in using the residuals of the fits of the cosmic muon tracks. The residual distribution in one view (wire or strip) is evaluated as the difference distribution between the hit position in that view and the position at which the track connecting the hits crosses the module in this view. Fig. 15 gives an example of how this procedure is applied. The residual distributions obtained for the middle module in the two views are shown. The *sigma* of the distributions represents a measure of the uncertainty in the geometry determined by data analysis.

The potential of this method cannot be fully utilized in the specific case of the MTD because there are only three modules for the determination

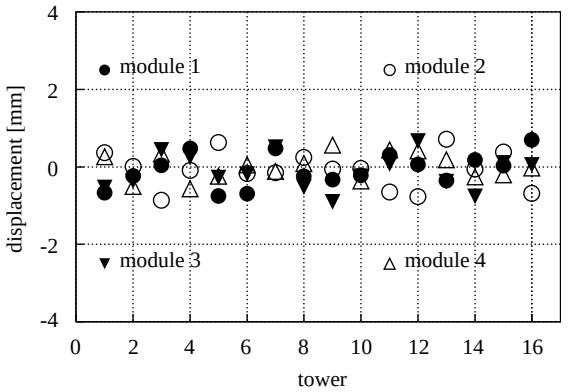

Fig. 14. Mean values of distributions of distances between X, Y crossing point and the nearest *diagonal strip* for all modules (top(1), middle(2), bottom(3), wall(4)).

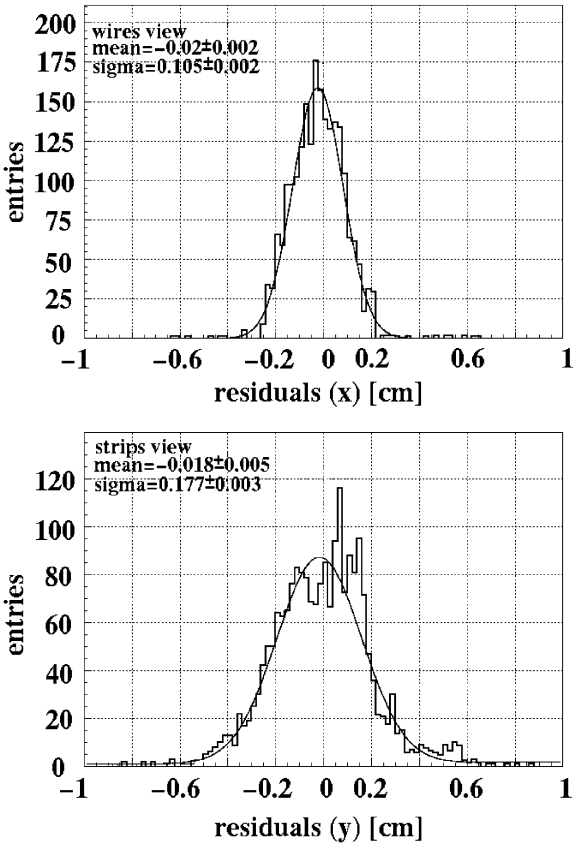

Fig. 15. The residual distributions for the middle module. The top panel shows the X-view while the bottom panel shows the Y-view.

of a track. In fact, it is possible to run into a systematic tilt of a tower. If, for example, the *correct* track is vertical, the bottom module precisely localized with respect to the floor of the tunnel, but the top module in the geometry DB is shifted to the right, then two indistinguishable solutions are possible: either to shift the top module to the left (correct) or to shift the middle module to the right (wrong).

However, this method can be used to reduce the spread of the distribution of the residuals and to improve the geometry DB and the intrinsic angular resolution without changing the reconstructed direction of the tracks. It can be applied to shift only one module, e.g. the middle one, in each tower using the top and the bottom modules as reference. The possible systematic tilt of the towers has to be checked and (if necessary) eliminated with other techniques.

6.1.4. Alignment checks with respect to the scintillator array

A modification of the previous method, that can be adopted in the case of KASCADE, consists in using the direction of the reconstructed shower from the scintillator array. In this case only one module is needed (for example, the middle one) for track identification, because the direction is fixed by the shower axis. Next, the distributions of the residuals in the different views of the top and bottom modules are analysed. Application of this method takes into account that muons in air showers are produced at a certain small angle with respect to the shower axis. This is a symmetric effect in the shower reference system. For checking the detector geometry one has to conserve this circular symmetry by choosing only showers reconstructed in a circular area around each tower. Moreover, the distribution of the shower core positions in this ring area should be uniform. Another source of uncertainty is the accuracy in the reconstruction of the shower direction from the scintillator array. Systematic errors, dependent on the position of the core of the shower inside the array, can mimic misalignment between the two detectors.

Applying this method a mean angle deviation of the MTD with respect to the scintillator array was deduced. It amounts to $<0.1^\circ$ in the X view and to 0.2° in the Y view. The misalignment in the X view is within the errors of the measurement while the deviation in the Y view might be a result of a systematic tilt and has stimulated further investigation. This example shows how the described method can be used to subsequent mutual tuning of both detector systems in the KASCADE experiment.

6.2. Angular resolution

6.2.1. Intrinsic angular resolution

The MTD has a *geometrical* resolution defined by its design and dimensions. With 820 mm spacing between each horizontal module in the towers, 10 mm ST wire spacing and 20 mm strip pitch the mean value of the geometrical resolution is about 0.35° for vertical muons and improves with increasing zenith angle. The dependence on the zenith angle of the track is due to the change in effective extensions for wire cells and strips, as *seen* by the track, which decrease with the increase of the zenith angle. At the same time, the distance of flight between two modules in the detector increases. This geometrical resolution is known with certain errors, due to finite accuracy of the geometry determination (see Section 6.1). Full *intrinsic* resolution, which can be achieved by the MTD in determination of the muon directions, has to take into account also other effects.

An estimation of the full resolution and its dependence on the zenith angle has been obtained using a simulation of the MTD that takes into account its geometry DB and physical processes connected with the interactions of the particles in different materials of the detector, including the tunnel shielding. The simulation used the Cosmic Ray Event Simulation (CRES) MC program. CRES is a GEANT 3.21 [36] based program package, developed for the KASCADE detector simulation. The sample of muons used as input particles for the code has been chosen in such a way, that it reproduces the zenith and the azimuth distributions of shower muons with a realistic shower energy spectrum [37].

The resulting distribution of the difference between the muon direction above the tunnel

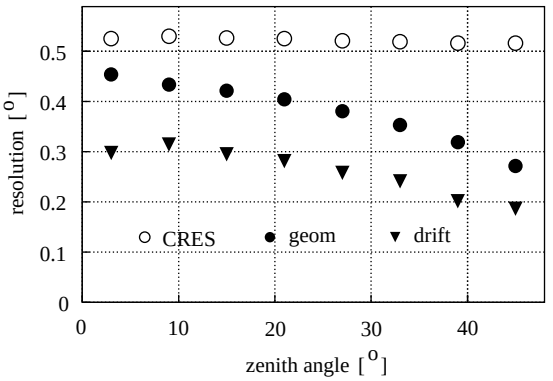

Fig. 16. Simulated angular resolution of the MTD, based on paired ST wire cells (open symbols) and separate ST cell and drift time information (filled symbols).

shielding and the reconstructed muon direction is histogrammed. The angle difference value, below which there is 68% of all events, we call *full intrinsic angular resolution* of the MTD. It is represented by the open circles in Fig. 16. The quoted values take into account, that in the main application of the MTD, namely investigation of the MPH, one should consider only high-energy muons ($E_\mu > 10$ GeV) produced high in the atmosphere, having less deflection from the shower axis.

However, one can raise the quality of the full intrinsic angular resolution by improving the geometrical resolution. Up to now, two ST wire cells are combined to reduce the number of readout electronic channels. The comparatively large anode wire signals allow a resistor network for every second wire on the adapter board (see Fig. 1), providing cell separation by means of the charge amplitude. Allowing for single cell readout and measuring the electron drift time [38], one can obtain the geometrical resolution down to the level of 0.2° (or even better) as shown in Fig. 16 for original and modified detector configurations. The filled symbols in Fig. 16, employing individual ST cells, do not take into account scattering of the muons in the MTD shielding. The intrinsic angular resolution of the real MTD must also cover the cases with varying cluster sizes on the strips and possible crosstalk in the electronics, which may worsen the quoted simulated numbers.

6.2.2. Twofold tracks

Measuring the angle between two assumed parallel muon tracks is a straightforward method of the determination of the angular resolution of a tracking detector. It is the only possibility in the case, where no other well-known reference direction is available. The width of this distribution is a measure of this resolution and shows the accuracy of angular track separation. High-energy muons in a shower can be, on average, assumed to be nearly parallel. However, this assumption is not fully valid because muons in a pair may originate from different production heights and may undergo different amount of scattering on their way, therefore, they may not be quite parallel. Furthermore, most muons in our data sample have energies close to the detector threshold (≈ 1 GeV). Nevertheless, this hypothesis allows to investigate the influence of various parameters which enter into the analysis. The angular resolution obtained that way can be used further to tune the MTD.

In our case this technique allows to test the orientation of individual towers with respect to the others and it is not influenced by systematic errors or asymmetries in the reconstruction introduced from the scintillator array. The drawback is that a large statistical sample is needed and that the method cannot be used to correct the relative orientation of the towers but only to observe it. In fact, it is not possible to identify which of the two towers is wrongly aligned and one can only align all the towers with respect to one of them. The cut in data used in this analysis selects events for which there are only two tracks in the full MTD with no more than one track in each tower. One of the tracks was required to be in tower 9 and the second in a different tower. In this way, tower 9 (near centre of the tunnel) has been used as the reference tower and the alignment of all the other towers has been checked with respect to it. The analysis demonstrates, that no tower shows in zenith and azimuth angles a misalignment with respect to tower 9 of more than 0.1°.

Studying the spatial distribution of twofold tracks in a low particle density environment, allows to investigate another important parameter of the MTD, namely the minimal spatial

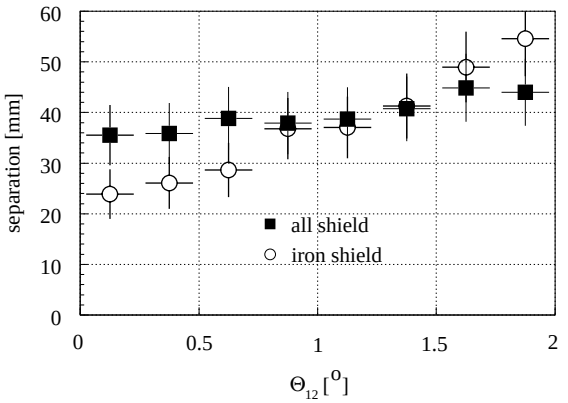

Fig. 17. Minimum spatial separation and relative angle between twofold tracks from anywhere above (full squares) and from the iron in the shielding (open circles).

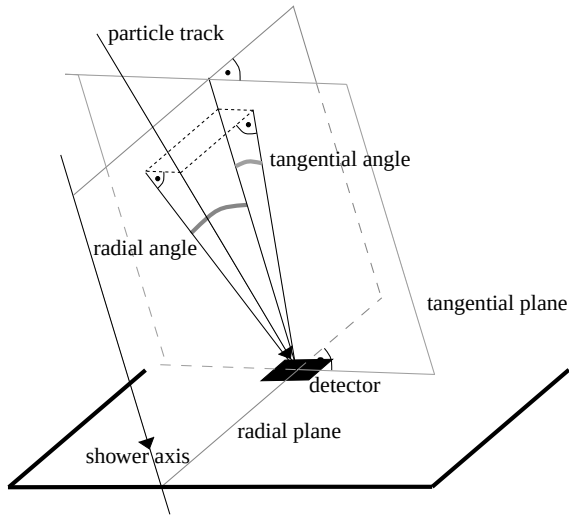

Fig. 18. Definition of *radial* and *tangential* angle between the shower axis and the measured track of a particle.

separation between two tracks in one tower. Twofold tracks appear in two classes, those which are already present in the shower above the MTD shielding and those, which originate from interactions within the absorber material. The internal trigger yields relatively more twofold tracks which can be traced back into the absorber. Inelastic cross-sections for incoming muons interacting with iron are of such order that they can account for the 2% fraction of twofold tracks over single ones. The second particle track is very likely made by a pion which had no time to decay. Fig. 17 shows the correlation between the minimum separation of tracks in a module and the relative angle between them. For two tracks which stem from all ranges of height (full squares), the minimal spatial separation is almost given by the cluster sizes as presented in Fig. 13. For the twofold tracks (open points) which can be traced back to originate in the iron absorber a steeper angular correlation can be expected because of the spatial confinement of the production target. Minimum separation can even become as small as the double ST cell size probably because of the spray of delta electrons accompanying the track coming out of the MTD shielding.

6.2.3. MTD versus array

Naturally, muons in air showers are not expected to be coplanar with the shower axis what leads to the concept of *radial* and *tangential* angles defined for the muon track with respect to the shower direction. The definitions of these angles, introduced in Ref. [39] and illustrated in Fig. 18, are defined by means of the radial and tangential planes. The radial plane is subtended by the shower axis and the line which connects the shower core with the position where the muon hits the array detector plane ($Z = 0$) above the MTD; while the tangential plane is orthogonal to the radial plane and parallel to the shower axis. The tangential angle τ, being of special interest for our purpose here, is the angle between the shower axis direction and the projection of the muon track onto the tangential plane.

While the radial angle is employed for the studies of the MPH [40,41], τ introduces some specific advantages for tracking checks. For the determination of angular resolution one has to consider the τ distribution. Any shift of the mean value of its τ distribution from zero is an indication of a systematic effect in the array-MTD reconstruction and can be used for mutual tuning of both detectors. The spread of this distribution depends on the multiple scattering of the muons and on the resolution of the two detectors, as well as on the transversal

displacement of the muon origin from the shower axis. An example of such a distribution is presented in Fig. 19. The measured τ distribution is fitted with two Gaussians and only the narrow component is considered to be associated with the resolution of the two detectors. The broad component, which contains only a few percent of the total number of events may be attributed to possible interactions of the muon in the MTD shielding and deserves further investigation. CORSIKA simulations show, that the spread of the τ distribution of high-energy muons is very small. Therefore, restricting the muon sample to very small τ values enriches the fraction of high-energy muons.

Operating the MTD one is interested in its accuracy in pointing at the sky. To study this quantity one needs a reference direction—shower axis. The following simple equation can be assumed to convert the RMS of the tangential angle distribution σ_τ to the angular resolution for a direction in the space: $\sigma_\Psi = \sigma_\tau\sqrt{2}$. This formula is the standard relation between the σ of a two-dimensional Gaussian distribution and the σ of its projection on a plane and has been checked by MC calculations to be valid within 5% in our experimental configuration.

The results of the analysis are shown in Fig. 20. The RMS of the angle difference distribution between the shower axis and the track in the MTD covers the directional resolution of both detectors

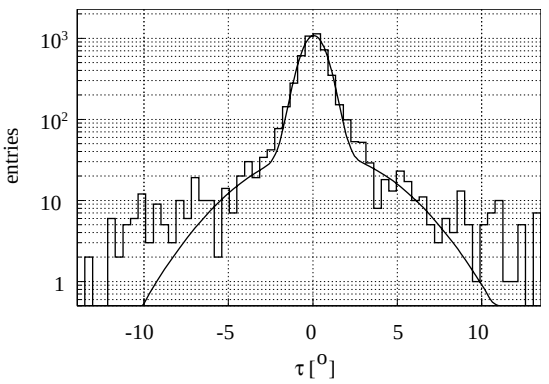

Fig. 19. Distribution of tangential angle τ between the shower axis and the particle track for a shower energy $E_0 = 10^{6.3}$ GeV fitted with a superposition of two Gaussians.

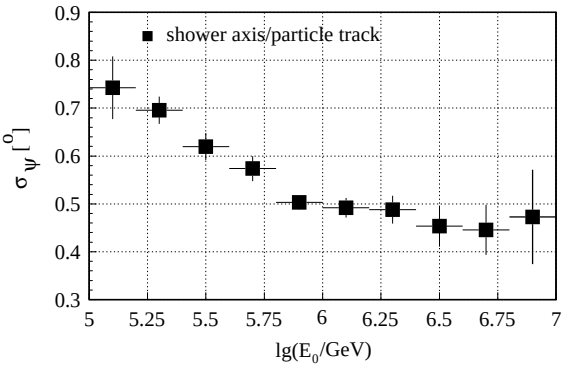

Fig. 20. The RMS (σ_Ψ) of relative angles between the shower direction and one particle track as a function of shower energy.

(the reference is not perfect). One should take into account, that in these values the deflections of muons from the shower direction due to various physical processes are contained. As mentioned in Section 6.1.1 CORSIKA simulations show a mean effect of 0.3° from scattering of high-energy muons in the atmosphere. The decrease of σ_Ψ with increasing shower energy is mostly due to the improving array and the MTD resolution with increasing shower size. The asymptotic value in Fig. 20 looks promising for the MTD resolution, taking into account the muon scattering contribution mentioned above.

Recalling that the algorithms adopted for determination of the shower direction in the scintillator array are usually developed and tuned with MC, but not all systematic effects, due to an incorrect evaluation of the shower particles arrival times in the scintillation detectors, can be detected by using the array data alone. Therefore, such a combined analysis with the MTD is useful for tuning the array itself.

Muon multiplicities observed in the MTD are considered to provide valuable information on hadronic interactions in the air shower cascade. An example of combining the observables on the air shower, as determined from the scintillator array, with those given by the MTD is shown in Fig. 21. Here, we plot the mean number (multiplicity) of tracks recorded by the MTD as a function of shower energy. The mean values do not reveal, that the track multiplicity distribution

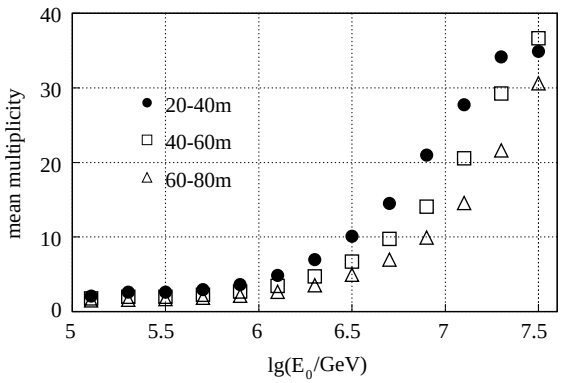

Fig. 21. Mean multiplicity of tracks recorded by the MTD as a function of shower energy for various shower core distances.

exhibits a tail up to 70–80 tracks. We allowed for very high shower energies to observe the effect of track multiplicity saturation for shower cores close to the MTD. Shower core distance intervals have been selected in the data analysis as quoted in Fig. 21.

Very energetic showers with cores close to the MTD lead to a saturation, which is probably due to the very high density of accompanying particles in the shower core leading to a poor track quality Q (see Section 6.1.1). The saturation occurs inspite of the finite minimal separation between twofold tracks as described above (see Section 6.2.2) and derived in low particle density environment. More effective track finding routines which will be developed in the future will allow to study higher densities of penetrating particles in the interesting region of high particle rapidities.

7. Conclusions

The paper has presented a detailed description of the MTD detector system. The specially developed ST chambers have been described together with the extensive tests after production. The influence of the environmental and design factors on the ST performance have been demonstrated and the results of various tests of the MTD were described. Finally, analyses to investigate the efficiency and angular accuracy of the MTD have been presented.

The introduction of the large MTD into the KASCADE experiment has significantly widened the multiparameter EAS analyses capabilities. The redundancy of information obtained with the scintillator array and the MTD can be used to find out systematic biases in the interpretation of the data. The presented results show satisfactory performance of the MTD in terms of stability and track recognition capability.

Future analysis of a larger data sample will provide more detailed information on the nature of high-energy shower muons. Triangulation will allow to investigate the MPH [40,41] and muon multiplicities, giving valuable parameters to derive the relative contributions of different primary cosmic ray particles. A natural extension towards even larger shower energies will be provided by KASCADE-Grande [42]. There is a common understanding that the high-energy shower muons serve as sensitive probes to investigate the high-energy hadronic interactions in the EAS development. Very inclined muons which can be studied when employing triggers performed with the wall modules are currently of vital interest.

Further investigations and improvements, both of the hardware and software, are in progress, with the aim to obtain the best angular resolution for the track direction. In future, the MTD will be upgraded by installing additional detector modules and a scintillator trigger plane providing the option of recording the electron drift time in the ST cells.

Acknowledgements

The authors would like to thank the members of the KASCADE collaboration, who contributed to the build up of the MTD: B. Hoffman, H. Hucker, H. Kern, G. Schleif, H. Skacel, F.K. Schmidt and H. Müller (Karlsruhe, Germany), P. Kleinwächter (Forschungszentrum Rossendorf, Germany), I. Atanasov (Institute for Nuclear Research, Sofia, Bulgaria) and J. Rachowski (University of Lodz, Poland). For valuable discussions and support we would like to thank G.D. Alekseev (Joint Institute of Nuclear Research, Dubna, Russia), M. Meoni (Pol. Hi. Tech, Carsoli, Italy), G. Mannochi and

P. Picchi (INFN, Italy), A. King and W. Flegel (CERN, Geneva, Switzerland) and L. Pinsky (University of Houston, USA).

This work was supported by the Forschungszentrum Karlsruhe. The partial support from the Ministry for Research of the German Federal Government within the collaboration agreement with Poland (WTZ POL 99/005) and from the Polish State Committee for Scientific Research (Grant No. 5 P03B 133 20) is gratefully acknowledged.

References

[1] L. Linsley, J. Phys. G: Part. Phys. 12 (1986) 51; L. Linsley, Nuovo Cimento C 15 (1992) 743.
[2] M. Ambrosio, et al., Nucl. Phys. B (Proc. Suppl.) 75A (1999) 312.
[3] H.O. Klages, et al. (KASCADE Collaboration), Nucl. Phys. B (Proc. Suppl) 52B (1997) 92; P. Doll, et al. (KASCADE Collaboration), Report FZKA 4686, Forschungszentrum, Karlsruhe (1990).
[4] O.C. Allkofer, P.K.F. Grieder, Physics Data 25-1 (1984) ISSN 0344–8401.
[5] J. Gress, et al., Nucl. Instr. and Meth. A 302 (1991) 368.
[6] L. Horton, et al., Nucl. Instr. and Meth. A 325 (1993) 326.
[7] M. Feuerstack, et al., Nucl. Instr. and Meth. A 315 (1992) 357; W. Rhode, et al., Nucl. Instr. and Meth. A 378 (1996) 399.
[8] O. Catalano, et al., Nuovo Cimento C 15 (1992) 759.
[9] S. Ahlenet, et al., (MACRO Collaboration), Nucl. Instr. and Meth. A 324 (1993) 337.
[10] G. Anzivino, et al., (LVD Collaboration), Nucl. Instr. and Meth. A 329 (1993) 521.
[11] C. Berger, et al., Nucl. Instr. and Meth. A 262 (1987) 463.
[12] P. Doll, et al., Nucl. Instr. and Meth. A 367 (1995) 120; I. Atanasov, et al., Report FZKA 6474, Forschungszentrum, Karlsruhe (2000).
[13] P. Doll, et al., Nucl. Instr. and Meth. A 342 (1994) 495; P. Doll, et al., Nucl. Instr. and Meth. A 323 (1992) 327.
[14] Pol. Hi. Tech., 67061 Carsoli (AQ), Italy.
[15] D. Hungerford, et al., Nucl. Instr. and Meth. A 286 (1990) 155.
[16] G.D. Alekseev, et al., Nucl. Instr. and Meth. A 243 (1986) 385.
[17] J.P. DeWulf, et al., (CHARM Collaboration), Nucl. Instr. and Meth. A 252 (1986) 443.
[18] E. Iarocci, Nucl. Instr. and Meth. A 217 (1983) 30.
[19] WATECH, Aslangasse 9/1/7, 1190 Wien, Austria.
[20] W. Bartl, Nucl. Instr. and Meth. A 305 (1991) 82.
[21] L. Pentchev, et al., Nucl. Instr. and Meth. A 399 (1997) 275.
[22] Little Falls Alloys, Paterson, NJ 07501, USA.
[23] J. Engler, et al., Nucl. Instr. and Meth. A 427 (1999) 528.
[24] Steiner Group, 57335 Erndtebrück, Germany.
[25] F. Beconcini, et al., Trans. Nucl. Sci. 35 (1988) 311; F. Beconcini, et al., Nucl. Instr. and Meth. A 227 (1989) 222.
[26] D. Adams, et al., (SMC Collaboration), Nucl. Instr. and Meth. A 435 (1999) 354.
[27] H. Leich, Transputer based VME Controller-TVC, Internal Report, IfH Zeuthen, 1991.
[28] SGS Thomson Microelectronics, Centro Dorezionale Colleoni, Palazzo ANDROMEDA 3, 20041 Agrate Brianza Milano, Italy.
[29] J. Zabierowski, P. Doll, Nucl. Instr. and Meth. A 484 (2002) 528.
[30] J. Zabierowski, et al., Nucl. Instr. and Meth. A 354 (1995) 496; J. Zabierowski, Report FZKA 5373, Forschungszentrum, Karlsruhe (1994).
[31] K. Daumiller, et al., Forschungszentrum, Karlsruhe (2002) to be published.
[32] D. Heck, et al., Report FZKA 6019, Forschungszentrum, Karlsruhe (1998).
[33] T. Antoni, et al., (KASCADE Collaboration), Astropart. Phys. 14 (2001) 245.
[34] R. Glasstetter, et al., (KASCADE Collaboration), Nucl. Phys. B (Proc. suppl.) 75A (1999) 238.
[35] J. Weber, Report FZKA 6339, Forschungszentrum, Karlsruhe (1999).
[36] GEANT Detector Description and Simulation Tool, Application Software Group, CERN, Geneva (1993).
[37] C. Caso, et al., (Particle Data Group), Eur. Phys. J. C 15 (2000) 1.
[38] R. Obenland, et al. (KASCADE Collaboration), Proceedings of the 27th ICRC 2001, Hamburg, Germany, Vol. 2, p. 814.
[39] K. Bernlöhr, Astropart. Phys. 5 (1996) 139.
[40] L. Pentchev, P. Doll, J. Phys. G: Nucl. Part. Phys. 27 (2001) 1459.
[41] C. Büttner, et al. (KASCADE Collaboration), Proceedings of the 27th ICRC 2001, Hamburg, Germany, Vol. 1, p. 153.
[42] M. Bertaina, et al. (KASCADE-Grande Collaboration), Proceedings of the 27th ICRC 2001, Hamburg, Germany, Vol. 2, p. 792.